ISSN: 2688-8645

Formation Control of Quadrotor UAVs

Haoran Wang[1, 2], Yi Luo[1, 2], Jun Zhao[1, 2], Zhanghuang Guo[1, 2]

[1]Sichuan University of Science & Engineering, Yibin 644000, China

[2]Sichuan Key Laboratory of Artificial Intelligence, Yibin 644000, China

Abstract

In recent years, the rapid development of quadrotor unmanned aerial vehicles (UAVs) has resulted in their widespread applications across various scenarios. However, single UAVs encounter multiple challenges during mission execution. Consequently, an increasing number of tasks are being conducted in the form of UAV formations. This paper focuses on quadrotor UAVs and proposes a formation control scheme that can be validated through simulation and experimentation. The research begins with the dynamic modeling of quadrotor UAVs and the design of an experimental platform for UAVs. The formation structure of UAVs is then developed based on the Leader-Follower theory, and a multi-type PID controller is employed to design the formation control algorithm.

Keywords

UAV; Multi-type PID; UAV Formation; Control Experiment.

1. Introduction

Unmanned aerial vehicles (UAVs) are unmanned flying devices that can be controlled programmatically or manually. Due to the development of control technologies and the decreasing cost of equipment, UAVs have found wide applications in both military and civilian domains [1-3]. Quadrotor UAVs, in particular, are capable of performing functions such as terrain-agnostic takeoff and landing, as well as hovering observations, even in complex environments. Based on these capabilities, they can accomplish tasks that are challenging for conventional UAVs in various everyday and specialized operational environments, resulting in higher utilization rates [5-6].

Formation control of unmanned aerial vehicles (UAVs) can be defined as the utilization of multiple UAVs to form a cohesive swarm or cluster in order to accomplish tasks that a single UAV alone cannot achieve. UAV formations offer numerous advantages in flight missions, including expanded operational range, reduced economic losses, and coordinated control information. This also highlights the advantages of studying multi-agent cooperation [9-11]. Enhancing the stability of UAVs in a multi-UAV system and achieving formation control can enhance the operational efficiency of quadrotor UAVs in various environments while reducing power consumption.

In this paper, an improved PID control algorithm is proposed to address the formation control of quadrotor UAVs. The algorithm tackles issues such as integral saturation and disturbance rejection that are typically encountered in traditional PID control algorithms. By applying the Leader-Follower theory, the algorithm achieves formation control of the UAVs. The designed quadrotor UAV formation control platform, based on the ROS system, is utilized to conduct both the formation control and experimental simulations of the UAVs. The simulation and experimental results demonstrate the validity of the proposed theory and the stability and feasibility of the designed control platform.

ISSN: 2688-8645

2. Formation Control of Quadrotor UAVs

2.1. Design of Formation Control Platform

The hardware structure of the UAV experimental platform can be divided into three main parts: the hardware configuration of the DJI Tello drones, the deployment of a local positioning server for quadrotor drones, and the deployment of the formation controller.

For the hardware configuration of the DJI Tello drones, a customizable computer is used to install the UAV-dedicated ROS2GO system. The ROS2GO system is used for UAV control configuration, such as establishing Wi-Fi connectivity between the drones, configuring control topics, and matching multiple UAVs. The hardware configuration based on the DJI Tello drones assigns a unique identifier to each experimental UAV, ensuring that there is no overlap or interference in the information transmission during the experiments. The transmission of control information has a dedicated channel to ensure the accuracy of control.

The deployment of the local positioning server for quadrotor drones primarily focuses on the localization control of the quadrotor drones. The NOKOV motion capture positioning system is used for this purpose. It is installed within the application range of the drones and calibrated with eight high-precision motion capture cameras. With this setup, each quadrotor UAV in the formation can be accurately located in real-time, and the data can be transmitted back.

The formation controller is deployed using one or more Jetson Nano controllers, responsible for real-time UAV localization information processing and algorithm execution. The processed mobility parameters of the UAVs are converted into corresponding rotor speeds for the quadrotor drones, which are then sent to each DJI Tello drone via the ROS2GO system. The Jetson Nano controller also receives a portion of the UAV information from Simulink, which uses MATLAB-ROS communication technology to publish real-time monitoring and compensation data within the local area network.

The main components of the quadrotor UAV hardware system are as shown in the Fig. 1.

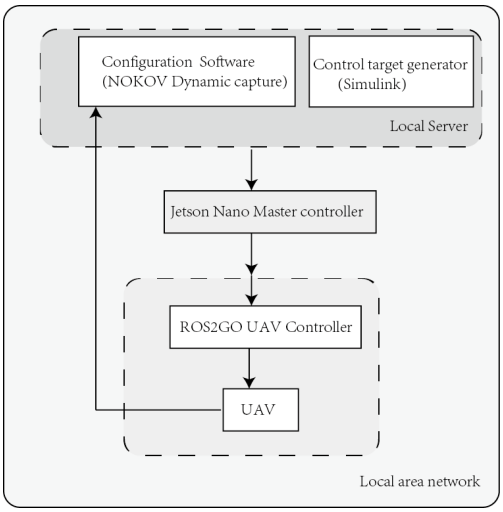

Fig 1. Overall hardware system architecture

The software design of the UAV experimental platform is divided into three main parts based on functionality: UAV position information acquisition, UAV control, and platform communication.

UAV position information acquisition is primarily responsible for analyzing and processing the position information of each UAV during the formation process. It captures the rigid body information of each UAV through the NOKOV motion capture device and generates specific rigid

ISSN: 2688-8645

body marker position information for each UAV. This marker position information is then preprocessed and sent to the Jetson Nano controller for analysis via network communication.

UAV control is primarily responsible for adjusting each UAV agent. It includes tasks such as takeoff and landing of the UAVs, trajectory tracking design, formation control protocol design, and formation parameter settings. Flight control is the core part of formation control in the experimental platform, as all formation control protocols are implemented through this software component.

Platform communication is mainly responsible for the transmission of control information between each UAV and the experimental platform devices. It involves setting up a network topology that allows communication between all experimental devices. Using ROS system's topic communication within the same local area network, each device can receive or publish relevant information, enabling closed-loop control of the UAVs.

The software control process for UAVs is shown in Fig.2

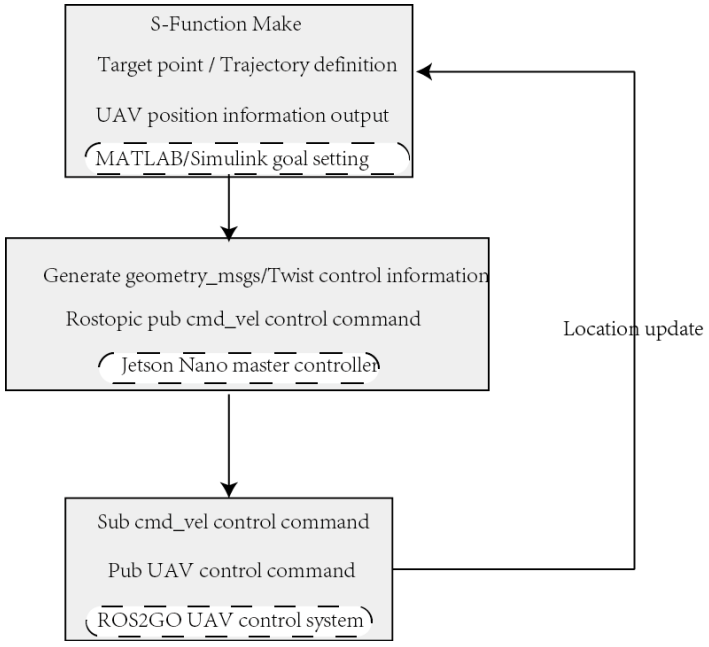

Fig 2. UAV control software process

2.2. Leader-Follower Formation Theory.

Based on the UAVs formation system structural model diagram shown in Fig.3, this research work establishes the following formation motion model. Since this study employs three UAVs, with one acting as the leader and the other two as followers, we will first analyze the case of one leader and one follower intelligent UAV, applying the same principles to the other follower UAV. Based on the research content of this paper, the formation control of the quadrotor UAVs is designed for motion in the horizontal plane (Plane XOY) and maintaining a constant altitude (Axis Z in the vertical direction). The motion equations are derived accordingly. Analyzing the coordinate systems of the leader and follower under the Leader-Follower formation theory, as shown in Fig.4 below.

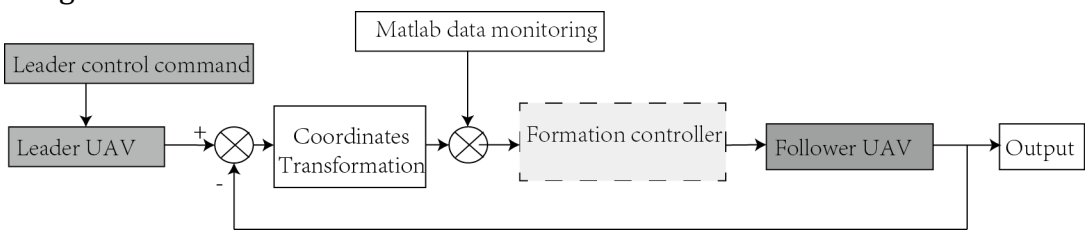

Fig 3. UAV Formation System Structural Model Diagram

ISSN: 2688-8645

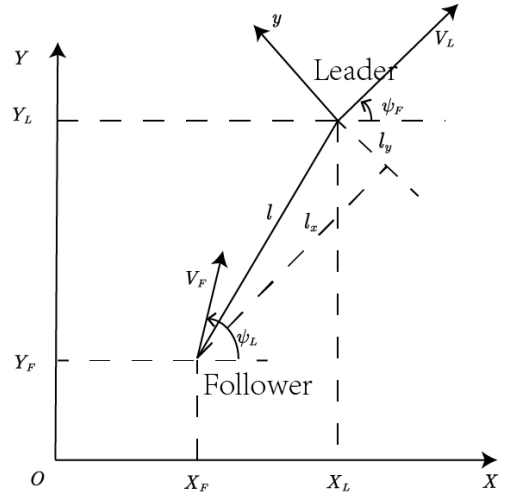

Fig 4. Horizontal leader-follower formation motion diagram

Based on the illustration in Fig.4, the motion model for the formation system in the plane can be described as follows:

$$\begin{bmatrix} \dot{x}_i \\ \dot{y}_i \\ \dot{\psi} \end{bmatrix} = \begin{bmatrix} \cos(\psi_i) & -\sin(\psi_i) & 0 \\ \sin(\psi_i) & \cos(\psi_i) & 0 \\ 0 & 0 & 1 \end{bmatrix} \begin{bmatrix} v_{ix} \\ v_{iy} \\ \omega_i \end{bmatrix} \tag{1}$$

In equation (1), v_{ix}, v_{iy} represents the velocity components of the quadrotor UAV in the XOY plane along the X-axis and Y-axis directions. ω_i represents the yaw rate of the quadrotor UAV, and $i = 1, 2, 3$ is the identifier for the intelligent UAV in the formation control system, with the leader designated as $i = 1$ and the follower as $i = 2, 3$. l, ψ represents the desired distance value and yaw angle between the leader and follower in the formation.

Assuming an inertial coordinate system, the coordinates of the leader and follower intelligent agents in the horizontal plane are denoted as (x_L, y_L) and (x_F, y_F), respectively. The distance value l_x, l_y between the leader and follower can be represented as a vector coordinate. Therefore, the following equation can be derived:

$$\begin{aligned} l_x &= -(x_L - x_F)\cos(\psi_L) - (y_L - y_F)\sin(\psi_L) \\ l_y &= (x_L - x_F)\sin(\psi_L) - (y_L - y_F)\cos(\psi_L) \end{aligned} \tag{2}$$

In (2)

$$\begin{cases} l_x = l\cos(\psi) \\ l_y = l\sin(\psi) \end{cases} \tag{3}$$

Derivate l_x, l_y to time, define $e_\psi = \psi_F - \psi_L$, and substitute it into Eq. (1) to obtain :

$$\begin{bmatrix} \dot{l}_x \\ \dot{l}_u \end{bmatrix} = \begin{bmatrix} l_y\omega_L \\ -l_x\omega_L \end{bmatrix} + \begin{bmatrix} \cos(e_\psi) & -\sin(e_\psi) \\ \sin(e_\psi) & \cos(e_\psi) \end{bmatrix} \begin{bmatrix} v_{Fx} \\ v_{Fy} \end{bmatrix} + \begin{bmatrix} -v_{Lx} \\ -v_{Ly} \end{bmatrix} \tag{4}$$

The formation error based on the leader-follower theory is defined as :

$$\begin{aligned} e_x &= l_x^d - l_x \\ e_y &= l_y^d - l_y \end{aligned} \tag{5}$$

The following dynamic error state space equation can be obtained by further derivation and collation of the formulas (5):

ISSN: 2688-8645

$$\begin{bmatrix}\dot{e}_x\\ \dot{e}_y\\ \dot{e}_\psi\end{bmatrix}=\begin{bmatrix}(-l_y^d+e_y)\omega_L+v_{Lx}\\ (l_x^d-e_x)\omega_L+v_{Ly}\\ -\omega_L\end{bmatrix}+\begin{bmatrix}-\cos(e_\psi) & \sin(e_\psi) & 0\\ -\sin(e_\psi) & -\cos(e_\psi) & 0\\ 0 & 0 & 1\end{bmatrix}\begin{bmatrix}v_{Fx}\\ v_{Fy}\\ \omega_F\end{bmatrix} \tag{6}$$

2.3. Design of UAV Multi-type PID Controller

Since the quadcopter UAV needs to map the rigid body coordinate system to the NOKOV dynamic capture system coordinate system when it moves in the NOKOV dynamic capture system, it is necessary to convert the UAV position information.

As shown in Fig.5, three optical dynamic capture balls are installed on the quadcopter UAV. The coordinate system of the three balls under the NOKOV dynamic capture system is shown in the figure.

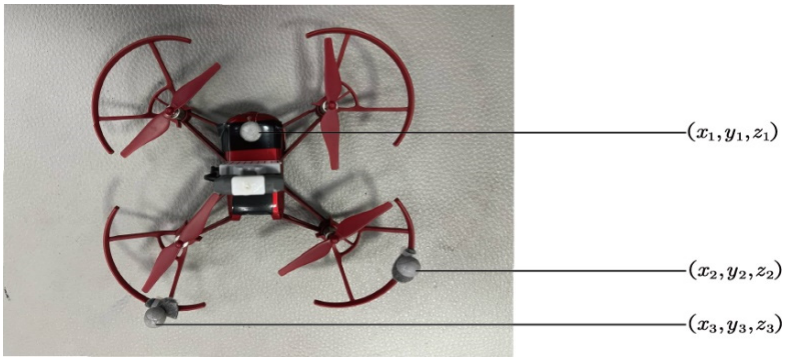

Fig 5. Schematic diagram of drone calibration ball

The analysis of the expected position:

$$\begin{bmatrix}x_d'\\ y_d'\end{bmatrix}=\begin{bmatrix}\cos\psi & \sin\psi\\ -\sin\psi & \cos\psi\end{bmatrix}\begin{bmatrix}x_{dw}\\ y_{dw}\end{bmatrix} \tag{7}$$

x_d', y_d' is the expected position of the UAV on the X-axis and Y-axis. Analysis of the actual position:

$$\begin{bmatrix}x'\\ y'\end{bmatrix}=\begin{bmatrix}\cos\psi & \sin\psi\\ -\sin\psi & \cos\psi\end{bmatrix}\begin{bmatrix}x_w\\ y_w\end{bmatrix} \tag{8}$$

x_d, y_d is the expected position of the UAV on the X-axis and Y-axis. The distance error expression of the quadcopter UAV based on the current position equivalent to the desired position can be expressed as:

$$\begin{bmatrix}e_x\\ e_y\\ 1\end{bmatrix}=\begin{bmatrix}\cos\psi & \sin\psi & -x_w\cos\psi-y_w\sin\psi\\ -\sin\psi & \cos\psi & x_w\sin\psi-y_w\cos\psi\\ 0 & 0 & 1\end{bmatrix}\begin{bmatrix}x_{dw}\\ y_{dw}\\ 1\end{bmatrix} \tag{9}$$

PID is a commonly used control method in the control system. Based on the PID controller of the UAV in this paper, the position PID is used. The flow chart is shown in Fig.6.

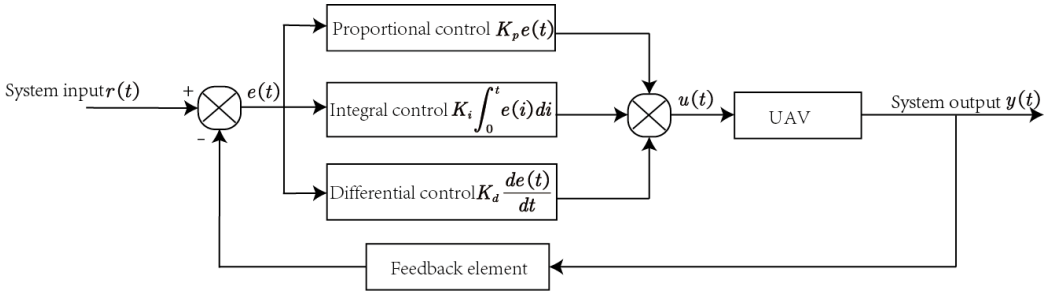

Fig 6. Basic structure of position based PID control process

The position PID control formula is shown as follows:

ISSN: 2688-8645

$$u(t) = K_p e(t) + K_i \int_0^t e(i)di + K_d \frac{de(t)}{dt} \tag{10}$$

According to the characteristics of the integral link of the UAV PID controller, a multi-type PID controller structure is designed as shown in Fig.7:

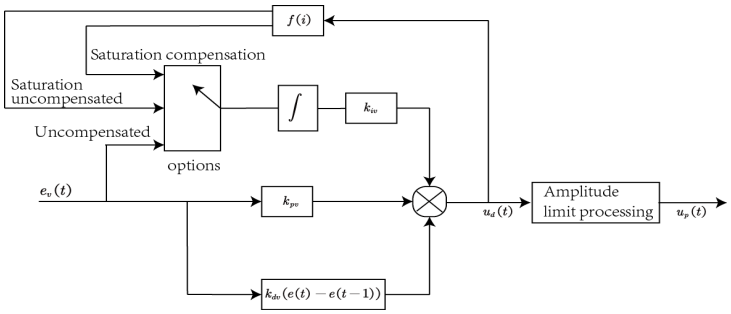

Fig 7. Structure diagram of multi-type PID controller

The variables in Fig.6 satisfy the following conditions:

$$u_d(t) = \begin{cases} k_{pv} e_v(t) + k_{iv} \int e_v(i)di + k_{dv}(e(t) - e(t-1)) & ,|u_d(t_-)| \leqslant \iota u_{\max} \\ k_{pv} e_v(t) + k_{iv} \int f(i)di + k_{dv}(e(t) - e(t-1)) & ,\iota u_{\max} < |u_d(t_-)| \leqslant u_{\max} \\ k_{pv} e_v(t) + k_{dv}(e(t) - e(t-1)) & ,|u_d(t_-)| < u_{\max} \end{cases} \tag{11}$$

In the above formula (11) $\iota \in (0,1)$ is constant value is determined by the characteristics of the UAV itself. When $|u_d(t_-)| \leqslant \iota u_{\max}$, the output of the controller system does not reach saturation; When $|u_d(t_-)| > \iota u_{\max}$, the output of the controller system reaches the integral saturation state, it needs to be processed.

The modules in (11) satisfy the following selection relations:

$$\begin{cases} f(i) = \begin{cases} e(i) = e(i) + i_\iota e(t), & \iota u_{\max} < |u_d(t_-)| \leqslant u_{\max} \\ 0 & , \quad |u_d(t_-)| > u_{\max} \end{cases} \\ e(i) = e(i)_{\max} & , \ e(i) > e(i)_{\max} \\ e(i) = -e(i)_{\max} & , \ e(i) < -e(i)_{\max} \end{cases} \tag{12}$$

3. Experiment and Analysis

The numerical simulation is carried out for the unmodified PID controller and the multi-type PID controller. The expected target value of the UAV is set to 1000, and the expected output error value is 0. Fig. 8 and 9 show the output of the system's expected target value and the output of the expected error within 1500 ms, respectively. In the simulation, a larger expectation of the system is introduced at 400 ms as a disturbance during the system operation.

As shown in Fig. 8, the multi-type PID controller improves upon the traditional PID controller. It exhibits accelerated convergence speed and lower overshoot value compared to the unmodified PID controller. The ability of the multi-type PID controller to restore the original value after interference, as seen by the control error added at 400 ms, is also stronger, indicating stronger anti-interference ability.Fig. 9 demonstrates that both the multi-type PID controller and the traditional unmodified PID controller exhibit improvements in the speed of the output error converging to 0 and the speed of re-converging to 0 after interference.

ISSN: 2688-8645

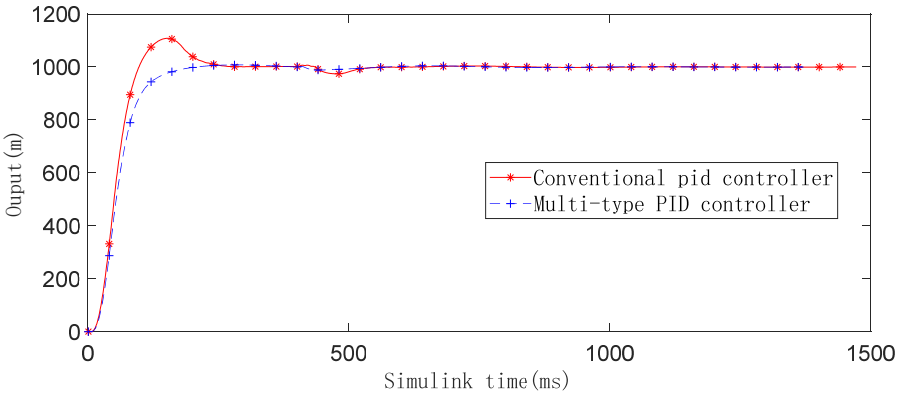

Fig 8. Comparison chart of algorithm output values between unchanged PID controller and multi-type PID controller

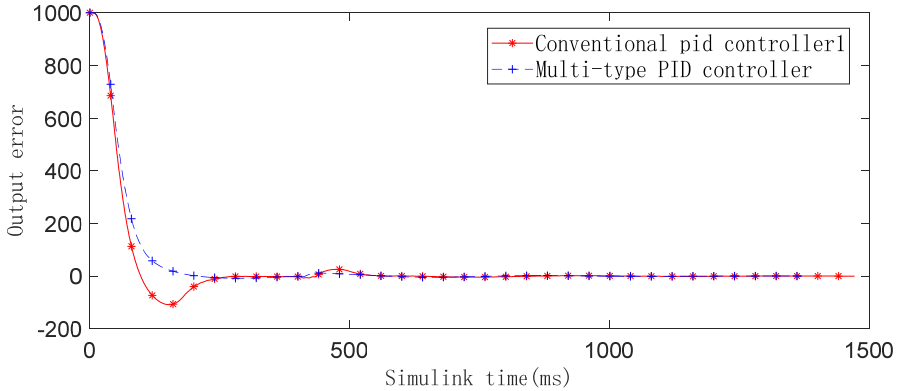

Fig 9. Comparison chart of algorithm errors between unchanged PID controller and multi type PID controller

The analysis of Fig.8 and Fig.9 confirms that the designed multi-type PID controller exhibits faster performance, improved stability, and better anti-interference effects. This provides evidence for its potential application in the formation control of quadcopter UAVs. The controller's superior performance contributes to a better formation control effect and a more stable formation.

Figures 10, 11, 12, and 13 provide an experimental analysis of quadrotor UAV formation. In Fig. 10 and 11, it is observed that the leader UAV1 initially deviates significantly from the reference trajectory. However, with the application of the control protocol, it eventually achieves stable tracking of the reference trajectory. The followers UAV2 and UAV3 establish a stable formation with the leader UAV1 under the influence of the formation control protocol. Fig.12 demonstrates that throughout the formation process, the formation shape between the followers and the leader remains consistent while maintaining a relative safety distance. The numerical values in the legend represent the distance error between the followers and the leader, indicating how closely they adhere to the desired formation. Fig. 13 depicts that despite the introduction of disturbances during the formation process, the formation control system effectively maintains stability. Over time, it achieves the desired formation shape, successfully completing the formation control task.

Fig.14 is a video screenshot showcasing three quadcopter UAVs successfully completing formation control. In Fig.14 (a), the screenshot captures the moment when three UAVs take off and form a specific formation structure in the air.

ISSN: 2688-8645

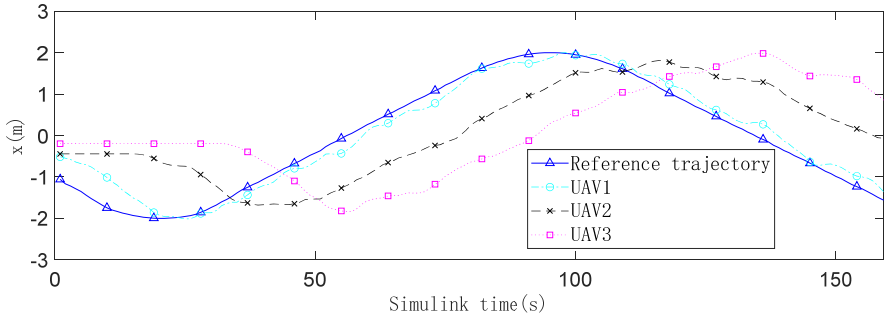

Fig 10. X-axis analysis diagram of formation experiment

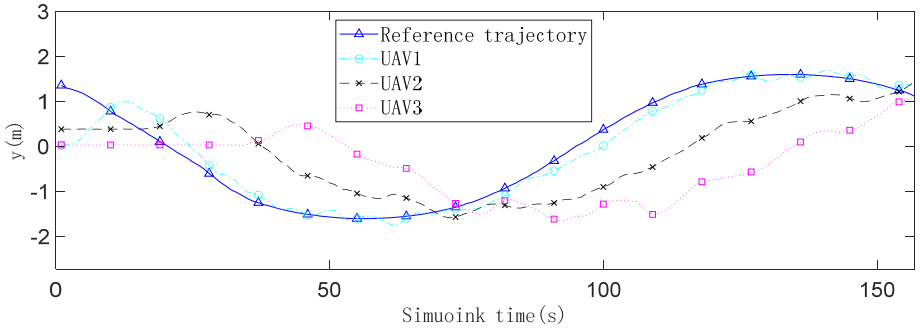

Fig 11. Y-axis analysis diagram of formation experiment

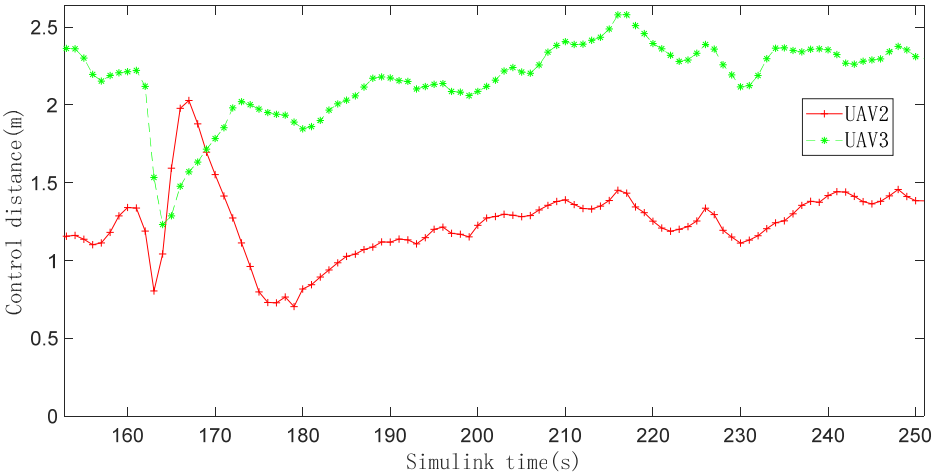

Fig 12. Formation stability analysis diagram of formation experiment

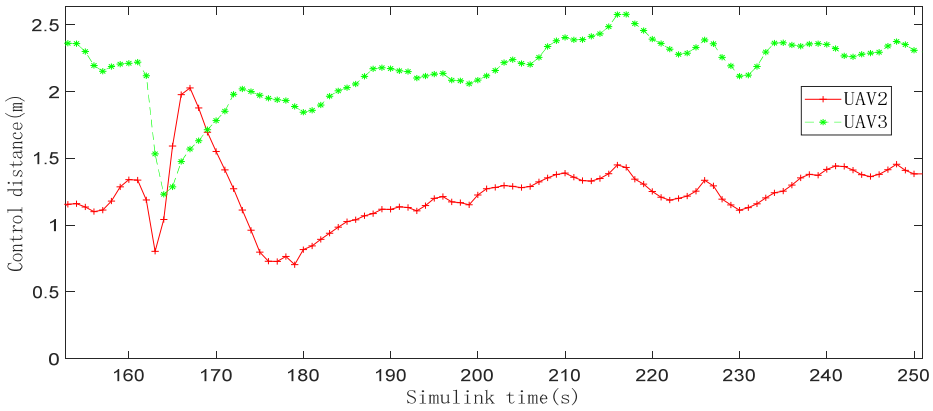

Fig 13. Interference recovery formation analysis diagram of formation experiment

ISSN: 2688-8645

The two follower UAVs closely surround the leader UAV. In Fig.14 (b), the leader UAV continues to maintain its piloting motion while the follower UAVs undergo formation transformation. Follower 2 is positioned behind follower 1 UAV to achieve the desired formation control. Fig.14 (c) demonstrates that the UAV formation remains in motion without disrupting the formation structure. Fig.14 (d) represents the initial formation state of the quadcopter UAV formation undergoing a formation switch. From Fig.14 (a) to Fig.14 (b), a stable formation control of the quadcopter UAV is established, and there is a closed-loop movement involving formation switching, showcasing stability and resistance to interference in the control process.

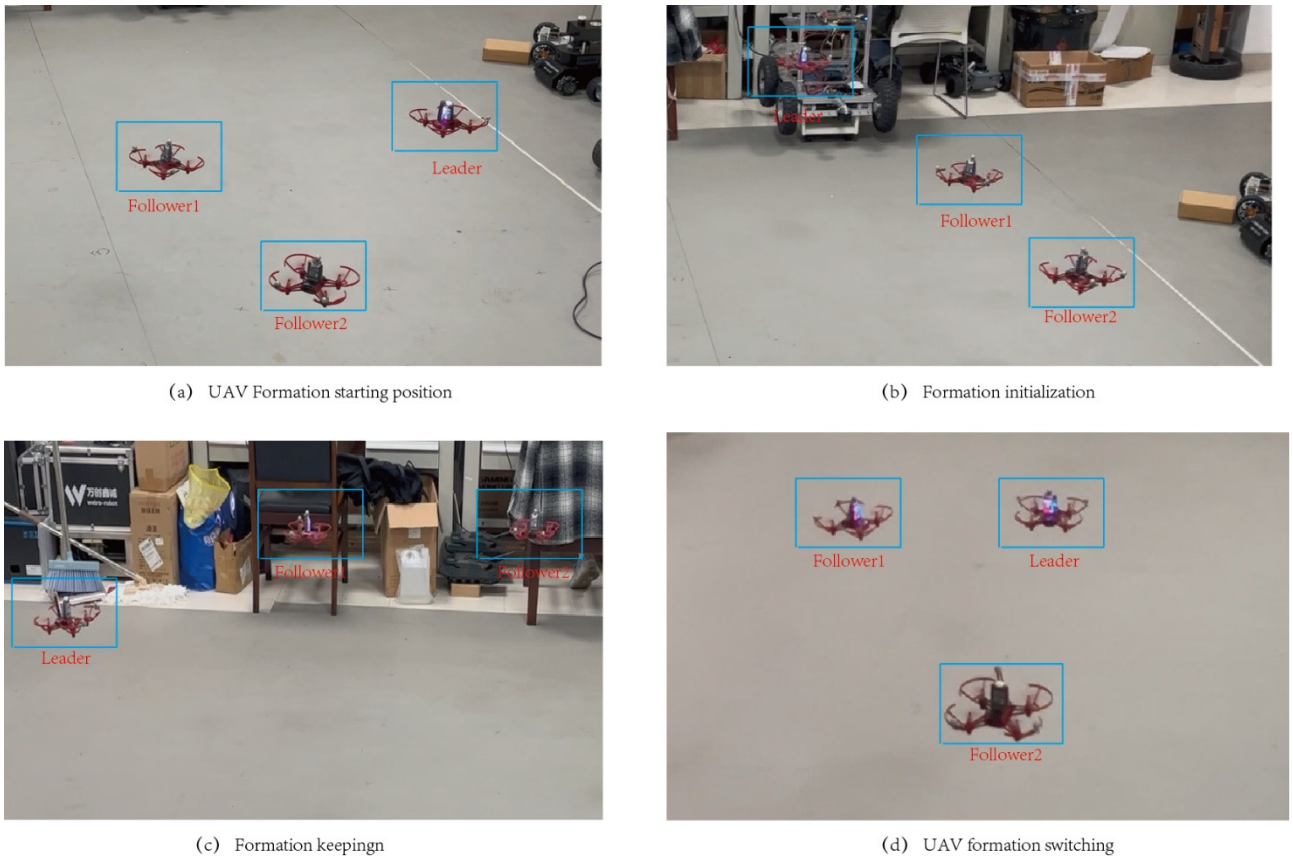

(a) UAV Formation starting position (b) Formation initialization

(c) Formation keepingn (d) UAV formation switching

Fig 14. UAV formation experiment screenshots

4. Conclusion

Due to the influence of PID integral error and the complexity of UAV formation control, the UAVs fail to achieve stable formation control. This paper addresses the issues of UAV formation model construction and PID controller design, and presents a designed process for UAV formation. Ultimately, stable formation control of the UAVs is achieved. Firstly, the theoretical model of the leader-follower formation is derived based on the formation structure, and mathematical descriptions and coordinate transformations are derived for the UAV formation shape. Subsequently, the position information of the UAVs is calculated based on the characteristics of UAV formation, and multiple types of PID controllers are designed for formation control. Finally, simulation and experimental results are provided. The simulation validation of the multiple types of PID controllers demonstrates their superior ability to prevent integral saturation and resist disturbances compared to traditional PID controllers. The UAV formation simulation verifies the feasibility of the dynamic model and formation controller. The UAV trajectory tracking experiment and formation experiment validate the feasibility and accuracy of the proposed theory.

ISSN: 2688-8645

References

[1] J. Tang, G. Chen and J. P. Coon. Secrecy Performance Analysis of Wireless Communications in the Presence of UAV Jammer and Randomly Located UAV Eavesdroppers[J]. IEEE Transactions on Information Forensics and Security, 2019, 14(11): 3026-3041.

[2] Z. T. Dydek, A. M. Annaswamy and E. Lavretsky. Adaptive Control of Quadrotor UAVs: A Design Trade Study With Flight Evaluations[J]. IEEE Transactions on Control Systems Technology, 2013, 21(4): 1400-1406.

[3] B. Tian, L. Liu, H. Lu, Z. Zuo, Q. Zong and Y. Zhang. Multivariable Finite Time Attitude Control for Quadrotor UAV: Theory and Experimentation[J]. IEEE Transactions on Industrial Electronics, 2018, 65(3): 2567-2577.

[4] R. Ji, J. Ma and S. Sam Ge. Modeling and Control of a Tilting Quadcopter[J]. IEEE Transactions on Aerospace and Electronic Systems, 2020, (56)4: 2823-2834.

[5] Q. Shao, R. Li, M. Dong and C. Song. An Adaptive Airspace Model for Quadcopters in Urban Air Mobility[J]. IEEE Transactions on Intelligent Transportation Systems, 2023, 24(2): 1702-1711.

[6] K. D. Sebesta and N. Boizot. A Real-Time Adaptive High-Gain EKF, Applied to a quadcopter Inertial Navigation System[J]. IEEE Transactions on Industrial Electronics, 2013, 61(1): 495-503.

[7] J. S. Bellingham, M. Tillerson, M. Alighanbari and J. P. How. Cooperative path planning for multiple UAVs in dynamic and uncertain environments[C]. Proceedings of the 41st IEEE Conference on Decision and Control, 2002, 3: 2816-2822.

[8] B. Zhou, H. Xu and S. Shen. RACER: Rapid Collaborative Exploration With a Decentralized Multi-UAV System[J]. IEEE Transactions on Robotics, 2023, 9(3): 816-1835.

[9] J. Wang, X. Zhang, X. He and Y. Sun. Bandwidth Allocation and Trajectory Control in UAV-Assisted IoV Edge Computing Using Multiagent Reinforcement Learning[J]. IEEE Transactions on Reliability, 2023, 2(2): 99-608.

[10] S. Rahim, L. Peng, S. Chang and P. -H. Ho. On collaborative multi-UAV trajectory planning for data collection[J]. Journal of Communications and Networks, 023, 25(6): 22-733.

[11] A. Hegde and D. Ghose. Multi-UAV Collaborative Transportation of Payloads With Obstacle With Obstacle Avoidance[J]. IEEE Control Systems Letters, 2022, 6: 926-931.